Single lane 176Gb/s Single Sideband PAM-4 Transmission over 400km with a Silicon Photonic Dual-drive Mach-Zehnder Modulator

Lei Zhang, Fan Yang, Xiaoke Ruan, Yanping Li and Fan Zhang*

State Key Laboratory of Advanced Optical Communication System and Networks

Frontiers Science Center for Nano-optoelectronics, Department of Electronics, Peking University, Beijing 100871

Author e-mail address: fzhang@pku.edu.cn

Abstract: We experimentally demonstrate ultra-high speed metro-scale optical transmission of SSB PAM-4 signal with a record single lane bit rate of 176Gb/s over 400km SSMF based on conventional silicon photonic dual-drive modulator with Mach-Zehnder structure.

1. Introduction

With the emerging applications such as cloud computing, the Internet of Things and virtual reality technology, the Internet traffic grows rapidly in medium/short-reach data center networks and metro networks. Recently, the IEEE P802.3bs Task Force has approved the 400-GE standards to meet the ever-growing bandwidth demands [1]. For the next generation optical interfaces of 400-GE, Optical transceivers with lane rate beyond 100G is a prominent and promising solution. In addition, silicon photonic (SiP) modulator also serves an attractive platform for the future metro-haul transmission due to its small footprint, low power consumption and complementary metal oxide semiconductor (CMOS) compatibility [2].

Direct detection technique has attracted significant attention owing to its low complexity and cost compared to coherent detection. However, for longer transmission distance, fiber chromatic dispersion (CD) will introduce severe power fading distortion to conventional double sideband (DSB) systems due to square-law direct detection [3]. For such scenario, single-sideband (SSB) pulse amplitude modulation (PAM) is proposed [4] as an alternative by removing one of the two conjugated sidebands. A demonstration of 280Gb/s/λ PAM-4 signals with optical band interleaving (OBI) technology transmission over 80km standard single mode fiber (SSMF) was reported in [5]. 102.4Gb/s/λ Nyquist SSB PAM-4 signal transmission over 720km SSMF with a bit error rate (BER) below the 20% soft-decision forward error-correction (SD-FEC) threshold of 2.4×10^{-2} was realized in [6]. 168Gb/s/λ SSB PAM-4 signal transmitting over 80km SSMF with a BER below 1.5×10^{-2} was demonstrated based on a silicon dual-drive traveling-wave Mach-Zehnder modulator (TW-MZM) [7].

In this paper, 176Gb/s/λ SSB PAM-4 transmission over 400km SSMF was experimentally demonstrated by using a silicon dual-drive TW-MZM with a 3-dB bandwidth of ~22.5GHz. The measured BER after transmission is below the 25% SD-FEC threshold of 4.0×10^{-2} [8] and the net bitrate is 139.1Gb/s (176Gb/s/1.25/51840×51200). To the best of our knowledge, it is the highest single-lane bit rate for C-band 400km SSMF SSB signal transmission based on a dual-drive SiP MZM and direct detection.

2. Modulator Characteristic and Experimental Setup

Fig. 1(a) shows the structure of the silicon dual-drive TW-MZM fabricated through IMEC's silicon photonics ISIPP50G technology. The GSGSG pads on the right side of lines are built for radio frenquency (RF) probe to apply the bias voltage and the high-speed driving signal. Light is coupled in and out of the waveguide device by fiber-to-chip grating couplers with an insertion loss of ~5 dB/coupler. Each arm of the MZM contains a phase modulator of 1.5 mm length, and the phase modulators operate via the plasma dispersion effect, where the depletion of free carriers from a reverse biased PN junction embedded in the waveguide causes a phase shift of the propagating light. Each signal line is terminated with a 25 Ω on-chip resistor, which is established by two parallel 50 Ω n-doped silicon slabs between the ground and the signal, to match closely with the characteristic impedance of the transmission line. The waveguides of the two arms are intentionally designed with 20μm length difference outside the modulation region, which allows the modulator's operation point to be adjusted through wavelength tuning. The measured electro-optic response of the MZM under different reverse bias voltages is shown in Fig. 1(b). We can see that the 3-dB bandwidth of the MZM gradually increases from ~15 GHz to ~22.5 GHz with the reverse bias voltage varying from 0 V to 2 V. We chose 1.5V as the reverse bias in the following tests.

The experimental setup and digital signal processing (DSP) diagram are depicted in Fig. 1(c). At the transmitter, an external cavity lasers (ECL) with ~100kHz linewidth is employed as the optical source. A polarization controller (PC) is applied to adjust the polarization state of the light coupling to the chip. The arbitrary waveform generator (AWG) (Keysight M8194A) operating at 120GSa/s generates a 88GBaud Nyquist SSB PAM-4 signal, which drives the on-chip silicon dual-drive MZM through a GSGSG probe with 40GHz bandwidth. Before launched into the 400km SSMF link, a polarization-maintaining erbium-doped optical fiber amplifier (PM-EDFA) is used to adjust the launch power. At the receiver, the signal is firstly amplified by an EDFA to compensate the fiber loss and then filtered by an optical band-pass filter (OBPF) (Yenista Optics XTM-50) to remove out-of-band noise. The signal is detected by a single-ended photodiode (PD) and subsequently amplified by an electrical amplifier (EA) both with a bandwidth around 50 GHz. The electrical signal is sampled by a real-time digital storage oscilloscope (DSO) (Keysight DSA-X 96204Q) operating at 160GSa/s to perform off-line DSP.

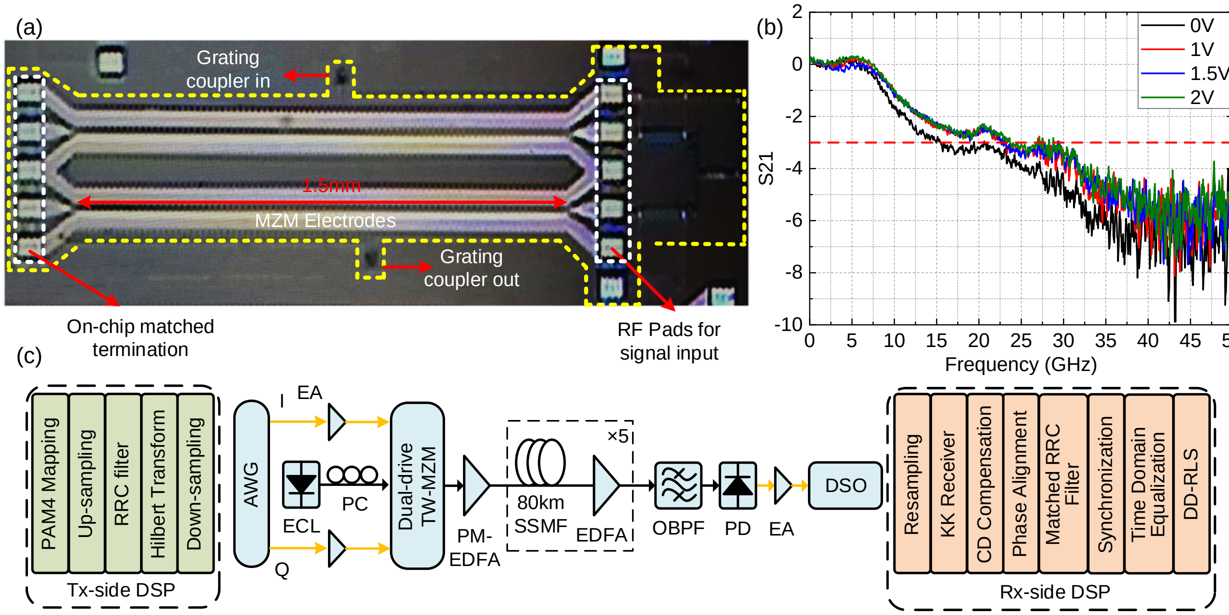

Fig. 1. (a) Micrograph and (b) Electro-optic response of the silicon dual-drive TW-MZM. (c) Experimental setup and DSP program. ECL: external cavity lasers; PC: polarization controller; TW-MZM: traveling-wave Mach-Zehnder modulator; AWG: arbitrary waveform generator; EA: electrical amplifier; PM-EDFA: polarization-maintaining erbium-doped fiber amplifier; SSMF: standard single-mode fiber; OBPF: optical band-pass filter; PD: photodiode; DSO: digital storage oscilloscope. Tx: transmitter; Rx: receiver; RRC: root raised cosine; DD-RLS: decision-direct recursive least square.

In the Tx-side DSP, the bit stream is mapped to PAM-4 first. After 15 times up-sampling, the signal is digitally shaped using a root raise cosine (RRC) filter with roll-off factor of 0.01. Then the signal is 11 times down-sampled. In the Rx-side DSP, firstly the signal is re-sampled to 4 samples per symbol. According to the previous work [9], The constant phase will be passed to the signal after PD detection as the second term in Eq.(1), and would not be removed by the Kramers-Kronig (KK) [10] receiver. Therefore, the phase alignment is required to shift the phase difference of the conjugated DSB PAM signal from 2φ to 0.

$$\left|C\exp(j\varphi)+S\right|^2=\left|C\right|^2+\mathrm{Re}\left\{C^*\cdot\left(S\exp(-j\varphi)\right)\right\}+\left|S\right|^2. \quad (1)$$

Therefore, after the KK receiver and CD compensation, the signal is rotated with a constant phase shifter to recover the original DSB signal [10]. After the matched RRC filter and synchronization, the signal is equalized with a $T_s/4$ (T_s means the symbol time period) spaced training sequence based time domain equalization. A finite impulse response (FIR) filter is extracted from the training sequence with the taps updated by the recursive least square (RLS) algorithm. Then a T_s spaced decision-direct recursive least square (DD-RLS) filter is used to improve the signal quality.

3. Experimental Results

We first optimize φ in the phase alignment operation [10] for 176Gb/s PAM-4 signal in back-to-back (BTB) and 400km transmission scenarios, respectively. As shown in Fig. 2(a), the optimal phase rotation angle is around 45°, which is reasonable for SSB signal [7]. Fig. 2(b) shows the measured optical spectrums of the transmitted, the received and the filtered signal at 0.02nm resolution. The carrier-to-signal power ratio (CSPR) is about 13 dB, which satisfies the minimum phase condition[9]. Fig. 2(c) shows the BER as a function of total launch power after 400km SSMF transmission. At the optimal launch power of 9 dBm, the BER is 3.51×10^{-2} that is below the 25% SD-FEC threshold of 4.0×10^{-2} [8]. The optical signal-to-noise ratio (OSNR) sensitivities at different transmission scenarios are shown in Fig. 2(d). It can be seen that there is 2.3 dB OSNR penalty for the signal after 400km SSMF transmission compared to the BTB results. Fig.2 (e) depicts BER dependence upon transmission distance at the launch power of 9dBm. Fig. 2 (f) and Fig. 2(g) display eye diagrams of 176Gb/s SSB PAM-4 signal after DD-RLS for BTB and 400km SSMF transmission scenarios, respectively.

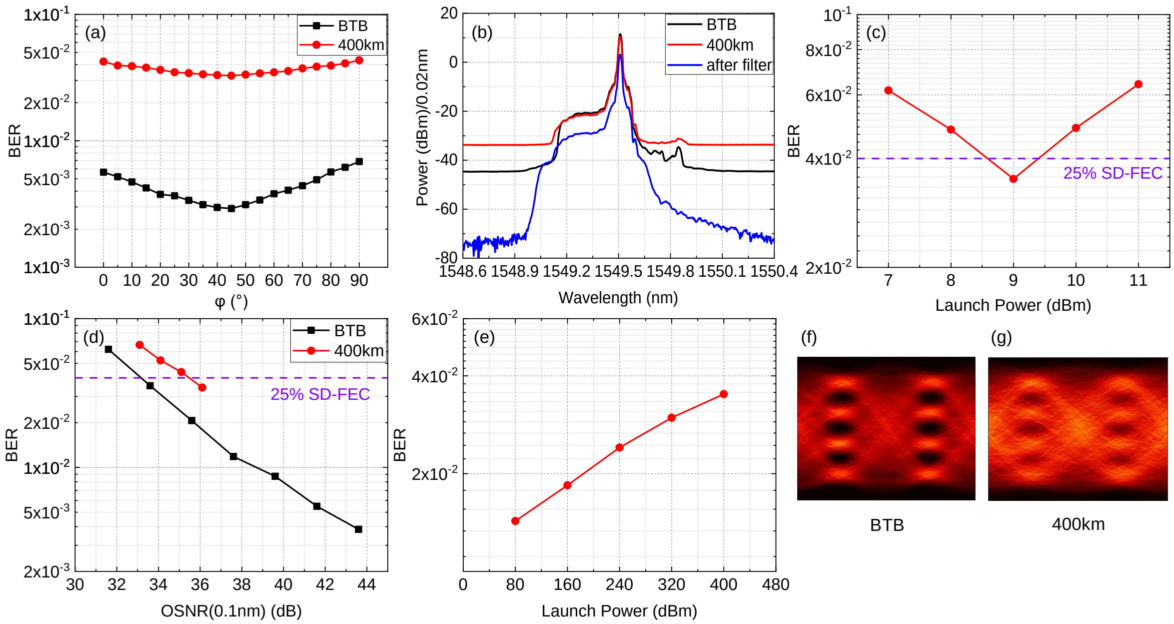

Fig. 2. (a) BER versus φ in the phase alignment operation for 176Gb/s PAM-4 signal. (b) Measured optical spectra. (c) Measured BER versus total launch power over 400km transmission. (d) Measured BER versus OSNR at different transmission scenarios. (e) Measured BER versus transmission distance with the launch power of 9dBm (f)-(g) Eye diagrams after DD-RLS for BTB and 400km transmission scenarios.

4. Conclusions

In this paper, we experimentally demonstrate 176Gb/s/λ SSB PAM-4 transmission over 400km SSMF by using a silicon dual-drive TW-MZM with a 3-dB bandwidth of ~22.5GHz. Thanks to the Rx-side DSP with the combination of training sequence based time domain equalization and DD-RLS, The measured BER after 400km SSMF transmission is below the 25% SD-FEC threshold. To our best knowledge, we report the highest single lane data rates for SSB signal with a SiP modulator in a metro-haul direct detection system.

5. Acknowledge

This work was supported by National Natural Science Foundation of China (No. 61535002), and in part by National Key R&D Program of China (No. 2018YFB1801204).

6. References

[1] IEEE P802.3bs 400 Gb/s Ethernet Task Force, accessed on Oct. 1, 2018. [Online]. Available: http://www.ieee802.org/3/bs/.
[2] L. Chrostowski, et al., Silicon Photonics Design: From Device to Systems (Cambridge University, 2015).
[3] Di Che, et al., J. Lightwave Technol., 34.2, 516-524 (2016).
[4] N. Kikuchi, et al., Proc. OFC 2016: Th2A.41.
[5] X. Wu, et al., Proc OECC 2019: ThC3-3.
[6] M. Zhu, et al., Optics Express, 26.6, 6629-6638 (2018).
[7] X. Ruan, et al., Photon. Technol. Lett., 31.7, 509-512 (2019).
[8] Son Thai Le, et al., J. Lightwave Technol., 37.2, 418-424 (2019).
[9] Y. Zhu, et al., Proc. OFC 2018: Tu2D.2
[10] A. Mecozzi, et al., Optica, 3.11, 1220-1227 (2016).